

Evaluation of mechanical and wear properties of hybrid aluminium matrix composites

T. RAJMOHAN¹, K. PALANIKUMAR², S. RANGANATHAN³

1. Sri Chandrasekharendra Saraswathi Viswa Maha Vidyalaya University, Enathur, Kanchipuram-631561, India;

2. Sri Sai Ram Institute of Technology, Chennai-600 044, India;

3. Department of Mechanical Engineering, Saveetha School of Engineering, Saveetha University, Chennai-602105, India

Received 6 September 2012; accepted 8 January 2013

Abstract: Hybrid metal matrix composites are important class of engineering materials used in automotive, aerospace and other applications because of their lower density, higher specific strength, and better physical and mechanical properties compared to pure aluminium. The mechanical and wear properties of hybrid aluminium metal matrix composites were investigated. Mica and SiC ceramic particles were incorporated into Al 356 alloy by stir-casting route. Microstructures of the samples were studied using scanning electron microscope (SEM). The chemical composition was investigated through energy dispersive X-ray (EDX) detector. The results indicate that the better strength and hardness are achieved with Al/10SiC–3mica composites. The increase in mass fraction of mica improves the wear loss of the composites.

Key words: hybrid metal matrix composites; SiC; mica; Al 356; stir casting; wear loss

1 Introduction

The increased demand of light weight materials with high specific strength in the aerospace and automotive industries has led to the development and use of Al alloy-based composites (mainly Al alloy/SiC composites). The metal matrix composites (MMCs) are slowly replacing the general light metal alloys such as aluminium alloy in different industrial applications where strength, low mass and energy savings are the most important criteria. The combination of various properties like electrical, mechanical, and even chemical can be achieved by the use of different types of reinforcements, i.e., continuous, discontinuous, short, whiskers, etc., with the MMCs [1]. The MMCs are attractive materials for use in structural applications because they combine favourable mechanical properties, good wear resistance, and low thermal expansion [2]. Particle-reinforced metal matrix composites (PMMCs) are very promising heterogeneous materials for structural applications due to their isotropic material properties, low cost, and ability to be formed using conventional

metal forming processes such as rolling, forging, and extrusion to produce the finished products. However, the indentation characteristics of heterogeneous material systems in various forms of composites, precipitation-hardened alloys, and dispersion-strengthened alloys are not known well. Their macroscopic indentation responses are affected by the mechanical properties of the matrix material and reinforcement as well as the type, shape, dimension, geometric arrangement, and volume fraction of the reinforcement [3]. Particulate-reinforced metal matrix composites have paved a new path to produce high strength and high wear-resistant materials by introducing hard ceramic particles and solid lubricant in the metal matrix [4]. Addition of ceramic reinforcements such as SiC, Al₂O₃, TiC, B₄C, and ZrO₂ to metal matrix improves hardness and thermal shock resistance [5].

Hybrid metal matrix composites (HMMCs) are second-generation composites where more than one type, shape, and sizes of reinforcements are used to obtain better properties [6]. Hybrid composites possess better properties compared with single reinforced composites as they combine the advantages of their constituent

reinforcements [7]. PRASAD and ASTHANA [8] reported that reinforcement of aluminium alloys with graphite solid lubricants and hard ceramic particles were used in automotive applications. DEONATH and ROHATGI [9] revealed that cast aluminium–mica particulate composites and copper-coated ground mica particles have enough strength and they are used as bearings in several applications.

JHA et al [10] reported that the addition of talc particles in the composite improves the wear resistance in the range of 22%–30% compared with the matrix alloy. RAJMOHAN and PALANIKUMAR [11,12] found that hybrid aluminium/ceramic–mica composites showed better machinability in terms of reduced thrust force, tool wear and burr height compared with aluminium/ceramic composites. 10% (volume fraction) SiC_p/Al–Mg composites with different Mg contents were successfully fabricated by semi-solid mechanical stirring technique under optimum processing conditions. The effects of Mg content on microstructure and mechanical properties were studied by scanning electron microscopy (SEM), X-ray diffractometry (XRD) and transmission electron microscopy [13]. It was found that the wear rate of 11% SiC MMC is higher on SiC abrasives compared with the 50% SiC MMC due to wear of the aluminium matrix. This trend is reversed on diamond abrasives due to pulling-out of the irregular shaped composite particles [14]. The yield strength and tensile strength increase, but the elongation decreases with the increase in the volume fraction of the SiC particles [15]. The addition of SiC particles in the form of composite powders by casting in semi-solid state decreases the SiC_p particle size, enhances the wettability between the molten matrix alloy and the reinforcements and improves the distribution of the reinforcement particles in the solidified matrix. It also increases the hardness and the impact energy of the composites and decreases their porosity [16]. The squeeze cast Al/SiC composite materials find enormous

applications in industry. Al₂O₃ fiber (Al₂O_{3f}) and SiC particle (SiC_p) hybrid metal matrix composites (MMCs) are fabricated by squeeze casting method [17]. The homogeneity of reinforcement and tensile properties increase with decreasing the stirring temperature and increasing the stirring time [18]. The hybrid SiC foam–SiC particles/Al double interpenetrating composites used as the brake materials of high-speed train were fabricated by squeeze casting technique [19].

The review of literature left the scope for the researcher to study the mechanical properties and wear loss of ceramic–mica reinforced hybrid composites. Moreover, adequate investigations have not been carried out to find the mechanical properties of hybrid Al/SiC–mica composites. In this study, SiC reinforcement is added to the Al356/mica composite to form stronger hybrid Al/SiC–mica composites. The mechanical and wear properties of Al356/SiC–mica composites are studied and presented in detail.

2 Experimental

2.1 Materials

Aluminium alloy, Al 356, was used as a matrix material and its chemical composition is presented in Table 1. The mechanical properties of Al 356 alloy is presented in Table 2. The silicon carbide particles with size of 25 μm and mica with average size of 45 μm were used as the reinforcement materials. The chemical composition of mica is presented in Table 3. The composites were fabricated with the mica particles of 0–6% in mass fraction in step of 3% and a fixed quantity of 10% of SiC.

The composites were fabricated by stir casting method to ensure uniform distribution of the reinforcements. The Al 356 alloy, which was in the form of ingot, was cut into small pieces to accommodate in the silica crucible. The mica for the study was procured from

Table 1 Composition of Al 356 alloy (mass fraction, %)

Cu	Si	Mg	Mn	Fe	Ti	Zn	Al
<0.0005	7.27	0.45	<0.002	0.12	0.08	0.005	Bal.

Table 2 Mechanical properties of Al 356 alloy

Density/ (g·cm ⁻³)	Ultimate tensile strength/MPa	Yield tensile strength/MPa	Elongation/ %	Modulus of elasticity/GPa	Poisson ratio
2.67	234	165	3.5	72.4	0.33

Table 3 Chemical composition of mica (mass fraction, %)

SiO ₂	Al ₂ O ₃	K ₂ O	Fe ₂ O ₃	Na ₂ O	TiO ₂	CaO	MgO
45.57	33.10	9.87	2.48	0.62	Traces	0.21	0.38

Premier Mica Company Chennai. Aluminum alloy was first melted in an electric furnace. Mica and SiC, preheated to a temperature of about 620 °C, were added to the molten metal at 750 °C and stirred continuously. The stirring was carried out at 500 r/min for 5–7 min. Magnesium was added in a small quantity during the stirring to increase the wetting. The melt with reinforcement was poured into a permanent metallic mould. The stir casting setup is presented in Fig. 1.



Fig. 1 Experimental setup used for stir casting

2.2 Experimental procedure

Microstructure and mechanical characterization of the composites were carried out. A metallographic examination was carried out using scanning electron microscope. The sample preparation for microstructural study was carried out first by polishing the sliced samples with emery paper up to 1200 grit size, followed by polishing with Al₂O₃ suspension on a grinding machine using velvet cloth. Finally, the samples were polished by using 0.5 μm diamond paste. Metallographic specimens of the composites were prepared for microstructural observation by grinding up to 600 grits with SiC abrasive paper and then consecutively polishing by diamond pastes of various sizes. The polished surface was etched with 10% NaOH solution and examined with a scanning electron microscope. The tensile properties of the specimen were measured by using an electronic tensile testing machine at room temperature based on ASTM standard. The cast composite specimens were machined using lathe to get the standard dimensions. Hardness tests were performed on composites to know

the effect of mica particles in the matrix materials. The polished composite specimens were tested for their hardness, using a Rockwell hardness testing machine having diamond indenter for 980 N load. Five sets of readings were taken at various places of the specimen and an average value was used for analysis. The chemical compositions of the different phases were investigated through spot and line-scan analyses on an energy dispersive X-ray (EDX) detector. The density of the composites was calculated theoretically by the rule of mixture using the following formula:

$$P_{th} = \rho_m \phi_m + \rho_r \phi_r \quad (1)$$

where ϕ_m and ϕ_r represent the volume fraction of the matrix and reinforcements respectively. The observed mechanical properties are presented in Table 4.

A pin-on-disc wear testing machine was used to evaluate the sliding wear behaviour of the composites. The wear tests were carried out under un-lubricated dry sliding conditions ((30±3) °C, RH 55%±5%) as per ASTM G99–95. The pin was initially cleaned with acetone and weighed accurately using a digital electronic balance. The independently controllable process parameters identified for the experimentation were: sliding speed (v), load (F), and mass fraction of mica (w). The selected process parameters, their notations, and their limits are given in Table 5. The disc material was made of EN-32 steel with a hardness of HRC 65.

3 Results and discussion

3.1 Microstructure

Figure 2 shows the SEM micrographs of Al/SiC-mica composites. The distribution of the SiC and mica particles in the aluminum matrix is noticeably uniform. Further, these figures reveal the homogeneity of the cast composites. Homogeneous distribution of the reinforcement in the matrix is essential to form a composite with uniform mechanical properties. The produced cast composites show some degree of porosity and sites of mica particles clustering. There is no large agglomeration of particles. Porosity may be due to improper casting or particles pulled out during grinding

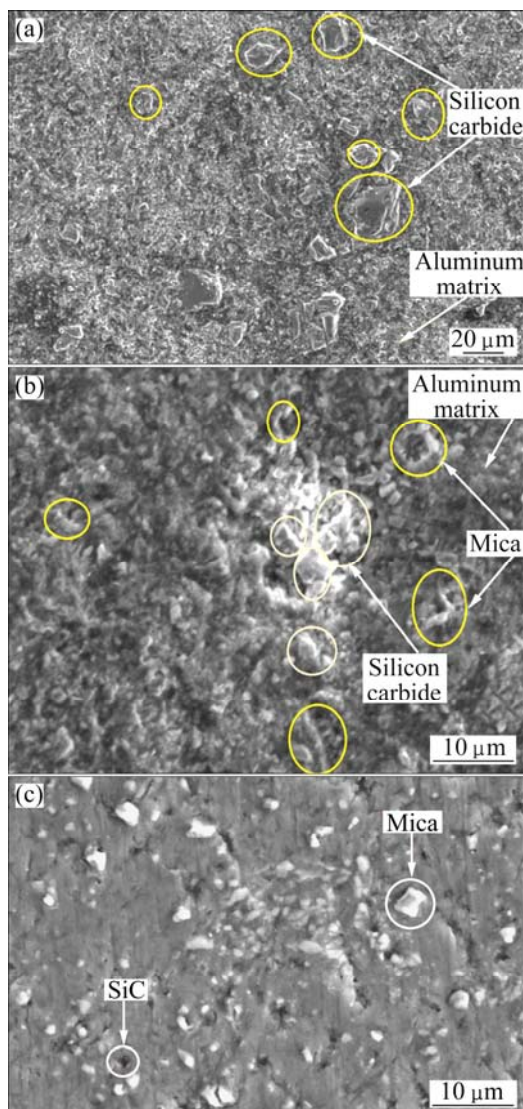
Table 4 Observed mechanical properties of composites

Composite	Tensile strength			Hardness			Density		
	Exp./MPa	Pred./MPa	Error/%	Exp./HRB	Pred./HRB	Error/%	Exp./($\text{kg}\cdot\text{cm}^{-3}$)	Pred./($\text{kg}\cdot\text{cm}^{-3}$)	Error/%
Al/10SiC	146	144	2.1	100	101	1.3	3	3.06	2.4
Al/10SiC–3mica	150	153	3.5	115	112	2.8	3.1	3.13	3.4
Al/10SiC–6mica	148	145	3.4	110	115	5.1	3.16	3.23	2.24

Exp.—Experimental value; Pred.—Predicted value.

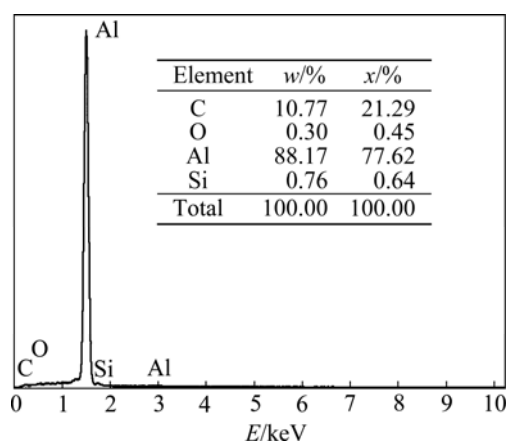
Table 5 Design of control parameters and their levels

Parameter	Symbol	Unit	Level		
			-1	0	1
Sliding speed	v	$\text{m}\cdot\text{s}^{-1}$	0.314	0.942	1.57
Load	F	N	9.81	29.43	49.05
Mass fraction of mica	w	%	0	3	6

**Fig. 2** SEM images of Al/10SiC composite (a), Al/10SiC-3mica composite (b) and Al/10SiC-6mica composites (c)

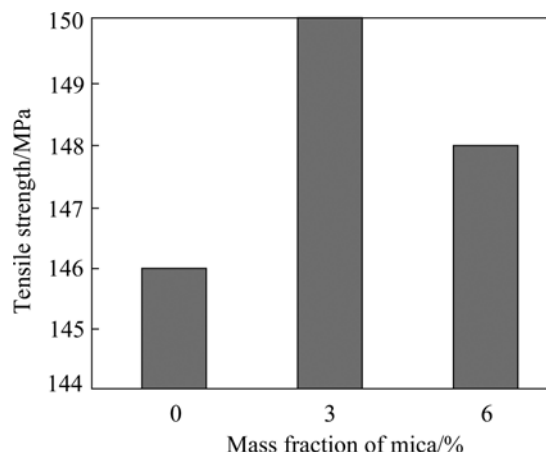
and polishing. Energy dispersive spectroscopy analysis of the Al/10SiC-3mica reinforced composite is shown in Fig. 3. From the figure it is clear that Al, O and C peaks are observed in the energy dispersive X-ray spectroscopy (EDS) analysis. The EDS analysis confirms that SiC and mica particles are present within the composites. Therefore, these SEM structures are evidence of successful incorporation of hybrid Al/SiC-mica composites. The clusters of SiC particles in the primary

Al seem to be finer. This can be explained by the fact that SiC particles have a lower thermal conductivity and heat diffusivity than aluminium melt and therefore, SiC particles are unable to cool down with the melt. As a result, the temperature of the particles is higher than that of the liquid alloy. The hotter particles may heat up the liquid in their immediate surroundings, and thus delay solidification of the surrounding liquid alloy. The SiC particles generally observed are accumulated in the interdendritic regions and geometrical trapping by dendrites is rarely observed. These observations suggest that the SiC particles are always pushed by dendrite fronts during solidification regardless of the dendritic arm spacing [20,21].

**Fig. 3** EDS spectrum of Al/10SiC-3mica composites

3.2 Tensile strength

The results obtained from the tensile tests of mica reinforced composites are shown in Fig. 4. The figure indicates that the composites reinforced with 10% SiC and 3% mica particle have the highest tensile strength of 150 MPa. At the same time, the tensile strength of composite with 10% SiC and 6% mica particle is found to be 148 MPa. The results indicate that with the increase

**Fig. 4** Tensile strength of composites with different contents of mica

in mass fraction of mica, the tensile strength of the composites increases up to certain value and then reduces. In the present investigation, addition of 3% mica shows better tensile strength than the 6% mica addition. For analyzing the proper strength, further investigations and sophisticated instrumentations are required.

3.3 Hardness

The results of hardness of the composites reinforced with different mass fractions of mica particles are shown in Fig. 5. The hardness value of Al/10SiC–6mica composite is less compared with Al/10SiC–3mica composite. Low values of hardness and strength are favorable for improving machinability, except for very ductile materials, which may generate a built-up edge, burr, and poor finish. Also, the lower the ductility is, the lower the energy required to shear the metal is and the less the shear forces are [22]. The hardness of the MMCs increases more or less linearly with the volume fraction of particulates in the alloy matrix due to the increasing ceramic phase of the matrix alloy.

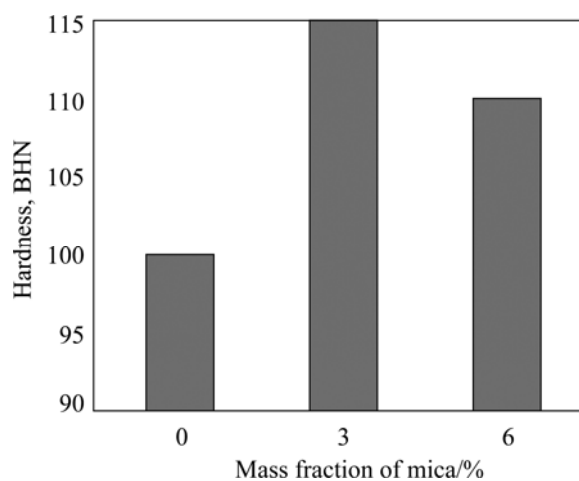


Fig. 5 Hardness of composites with different contents of mica

3.4 Density

The comparison of theoretical density obtained by the rule of mixture and experimental density obtained by Archimedean method for the composites is shown in Fig. 6. The result shows that the densities of mica reinforced composites are higher than those of ceramic reinforced composites. The results are in line with the result by SAHIN [23] who found that the density increased with increasing the volume fraction of particulates. The increase in density indicates that particle breakage may not have any significant influence on the composites. It is believed to achieve an improvement of the bonding between the particle and matrix.

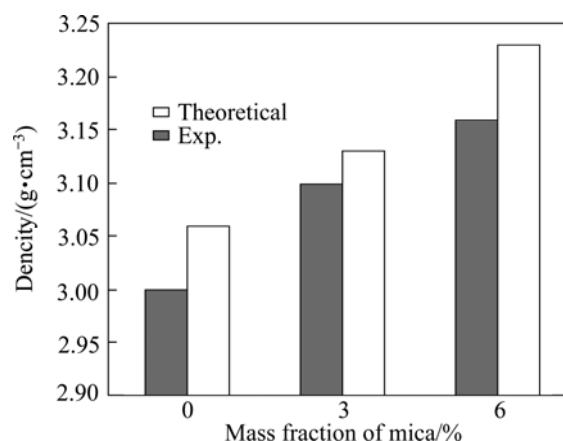


Fig. 6 Density of composites with different contents of mica

3.5 Wear loss

The experiments to analyze the wear loss have been carried out using central composite face centered second order design. In the current investigation, the number of variables considered is three and the number of experiments conducted is 20. The alpha value selected as per central composite design is 1. At the end of the each test, the pin is again weighed with the same balance after cleaning with acetone. The difference between the initial and final mass is a measure of wear loss. The observed responses, i.e., wear loss values for all the 20 experiments, are listed in Table 6.

For modeling the wear parameters with respect to the wear loss, response surface methodology was used. Usually, a second-order model was utilized in response surface methodology [11].

$$y = \beta_0 + \sum_{i=1}^k \beta_i x_i + \sum_{i=1}^k \beta_{ii} x_i^2 + \sum_{i,j} \beta_{ij} x_i x_j + \varepsilon \quad (2)$$

where β coefficients, which should be determined in the second-order model, are obtained by the least square method. The response surface methodology can be used to find the values of the controllable parameters that result in optimization of response or discover what values for the x values will result in a product (process) satisfying several requirements or specifications [11]. The second-order model is normally used when the response function is not known or nonlinear. In the present study, a second-order model was utilized. The wear loss in actual values is given by

$$\begin{aligned} \text{Wear loss} = & 1.64565 - 0.51733v + 2.04317 \times 10^{-4}F - \\ & 0.11634w - 9.85319 \times 10^{-4}vF + 5.77229 \times 10^{-3}vw - \\ & 4.31658 \times 10^{-4}Fw - 0.35233v^2 + 2.50142 \times 10^{-4}F^2 + \\ & 0.010116w^2 \end{aligned} \quad (3)$$

The adequacy of the developed model can be verified by using R^2 value after estimating the sum of squares (SS) and mean squares (MS).

Table 7 shows the analysis of variance carried out for wear loss with uncoded values. The F value in Table 7 indicates that the developed model is highly adequate at 95% confidence level. The diagnostic checking of developed model can be checked by residual analysis.

Residual is the difference between the observed values and the predicted or fitted values. The normal probabilities of residuals are shown in Fig. 7(a). From Fig. 7(a) it is clear that the data are spread roughly along the straight line. Hence, it can be concluded that the data

Table 6 Observed responses for wear loss

Exp. No.	Coded value			Actual setting			Wear loss/mg
	Sliding speed, v	Load, F	Mass fraction of mica, w	$v/(m \cdot s^{-1})$	F/N	$w/\%$	
1	-1	-1	-1	0.314	9.81	0	1.8
2	1	-1	-1	1.57	9.81	0	1.625
3	-1	1	-1	0.314	49.05	0	2.38
4	1	1	-1	1.57	49.05	0	2.14
5	-1	-1	1	0.314	9.81	6	1.458
6	1	-1	1	1.57	9.81	6	1.31
7	-1	1	1	0.314	49.05	6	1.92
8	1	1	1	1.57	49.05	6	1.74
9	-1	0	0	0.314	29.43	3	1.67
10	1	0	0	1.57	29.43	3	1.42
11	0	-1	0	0.942	9.81	3	1.53
12	0	1	0	0.942	49.05	3	2.03
13	0	0	-1	0.942	29.43	0	1.96
14	0	0	1	0.942	29.43	6	1.59
15	0	0	0	0.942	29.43	3	1.79
16	0	0	0	0.942	29.43	3	1.77
17	0	0	0	0.942	29.43	3	1.81
18	0	0	0	0.942	29.43	3	1.77
19	0	0	0	0.942	29.43	3	1.84
20	0	0	0	0.942	29.43	3	1.74

Table 7 ANOVA for wear loss

Item	Sum of square	Degrees of freedom	Mean square	F value	p -value prob> F	Note
Model	1.155963	9	0.12844	33.18025	< 0.0001	Significant
v	0.098605	1	0.098605	25.47281	0.0005	
F	0.618517	1	0.618517	159.7828	< 0.0001	
w	0.356077	1	0.356077	91.9861	< 0.0001	
vF	0.001176	1	0.001176	0.303831	0.5936	
vw	0.000946	1	0.000946	0.244414	0.6317	
vw	0.005151	1	0.005151	1.330701	0.2755	
v^2	0.05771	1	0.05771	14.90836	0.0032	
F^2	0.022343	1	0.022343	5.771798	0.0372	
w^2	0.019933	1	0.019933	5.149218	0.0466	
Residual	0.03871	10	0.003871			
Lack of fit	0.036027	5	0.007205	13.42604	0.0064	
Pure error	0.002683	5	0.000537			
Cor. total	1.194673	19				

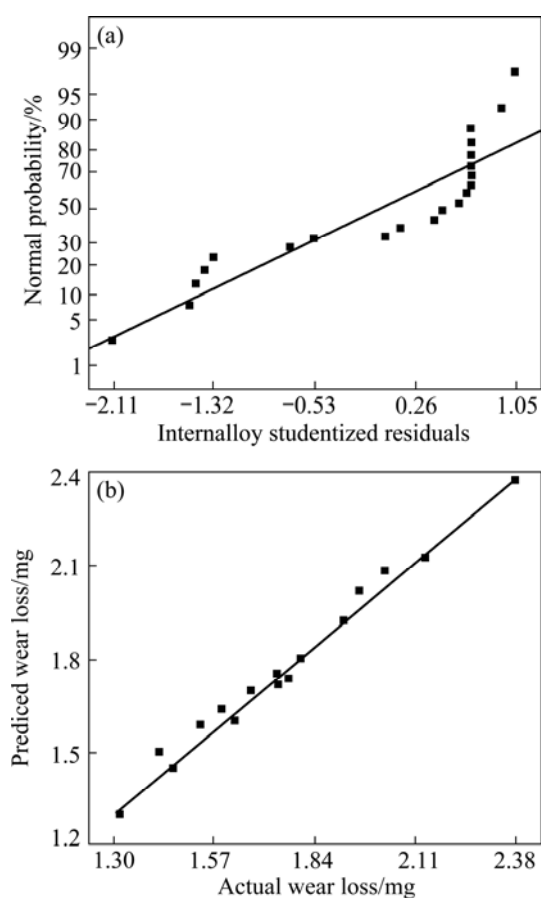


Fig. 7 Normal probability plot of residuals for wear loss (a) and predicted vs actual values (b)

are normally distributed. Figure 7(b) shows the predicted results against the actual results. From Fig. 7(b) it is asserted that the predicted results are very close to the experimental results and hence the response surface models are suitable for predicting wear loss of hybrid composites.

The variations of wear loss with sliding speed, load and mass fraction of mica are presented as 3D response graph in Fig. 8. From the analysis of the graphs, it can be concluded that the increase of load leads to a significant increase of the wear loss. The tribological behavior of a composite depends on the microstructural properties of the material and also on the type of loading-contact situation. According to Archard's theory, the amount of sliding wear is usually proportional to the applied load and the sliding distance and inversely proportional to the hardness of the surface worn away. Shearing of the asperity junctions can occur in one of the two bodies depending on the relative magnitude of interfacial adhesion strength and the shearing strength of surrounding local regions.

The effect of sliding speed shows a reasonable decrease of the wear loss. As for the effect of sliding speed on the wear loss in Figs. 8(a) and (b), it is

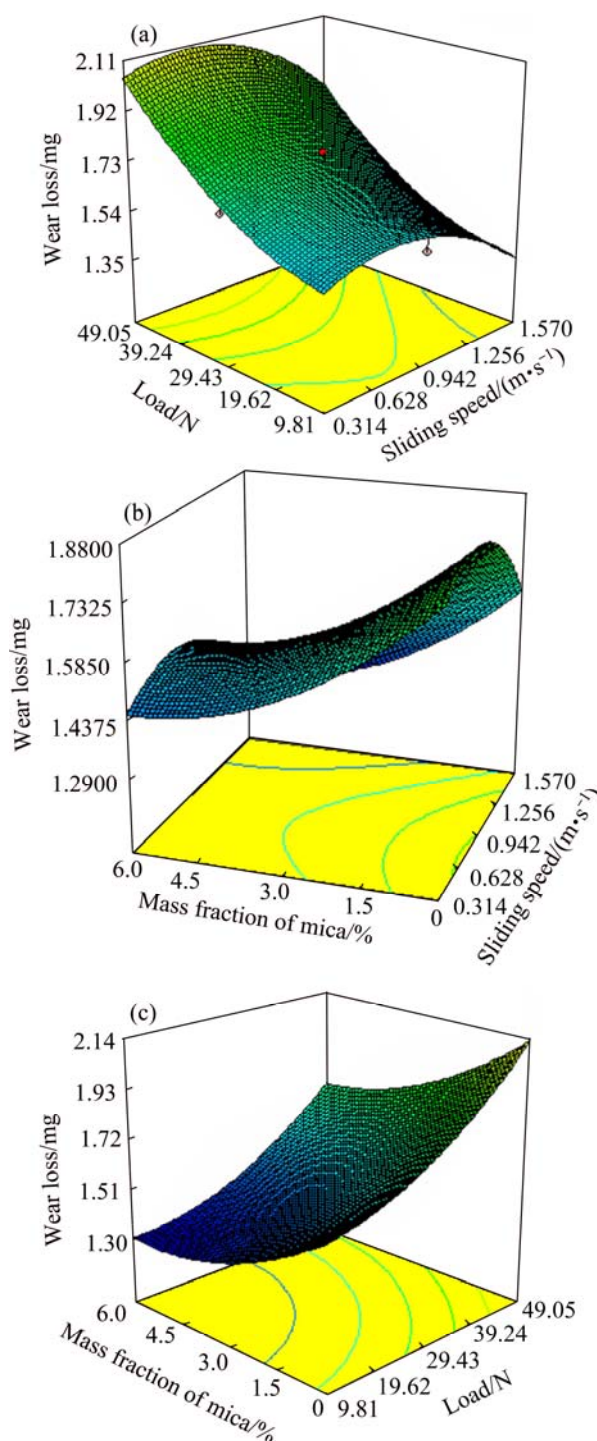


Fig. 8 3D response graph for wear loss: (a) Load vs sliding speed; (b) Mass fraction of mica vs sliding speed; (c) Mass fraction of mica vs load

indicated that at a constant load, the increase of speed causes more wear loss at the beginning, whereas the further increase of speed results in the decrease of wear loss due to the increase of interface temperature and softening of the composites. Most metals oxidize typically in air to form oxide film within a few minutes of exposure of the clean surface. Those films play a

crucial role in friction characteristics. At normal loads, the oxide films separate the two metals and the coefficient of friction is low because the oxide has low shear strength and its low ductility limits junction growth. At higher loads, the surface films deform and metallic contact occurs, leading to high coefficient of friction. The presence of oxide layer reduces the chance of direct metallic contact and therefore asperities interaction is reduced, which is a prerequisite for adhesive wear. Moreover, increasing the sliding speed also increases the interface temperature. High sliding velocities result in surface frictional heating, which, in turn, results in the formation of a thin molten layer at asperity contacts in the case of low melting of metals. The wear loss is less for mica reinforced composites even at high loads. The mechanically mixed layer (MML) formed is stable and able to withstand higher temperatures compared with other materials [24]. BASAVARAJAPPA et al [21] found that the graphite particles smear at the interface and reduce the coefficient of friction. Hence, the heat generated due to friction also reduced. In MMCs, MML is present and this layer exhibits hardness, approximately six times that of the bulk composite. So, the formation of work hardened layer between the pin surface and steel disc also reduces the wear rate as sliding speed increases. The solid lubrication film formed as a result of adding carbon fibers improves the wear resistance of carbon hybrid composites because this film reduces the high friction force between MMCs and counter material. At high sliding speed, localized melt and slip and large plastic deformations due to the high frictional heat are the dominant factors contributing to the removal of MMCs.

Figures 9–11 show SEM images of wear surface of the mica-reinforced composites. These micrographs show numerous long grooves and craters on worn surfaces with the increase of load to 49.05 N at sliding speed of 1.57 m/s. As the load increases, the wear behaviour of the composites changes from abrasion to delamination as evident from the SEM micrographs [25,26]. The rows of furrows and delamination are the

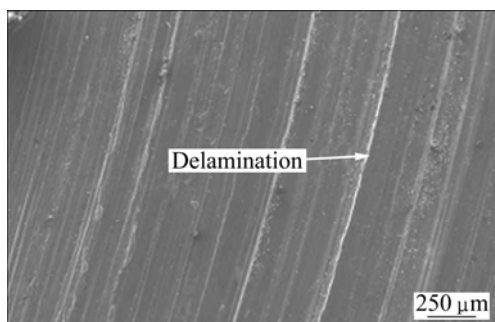


Fig. 9 Wear surface of composite with 3% mica reinforcement under load of 49.05 N and sliding speed of 1.57 m/s

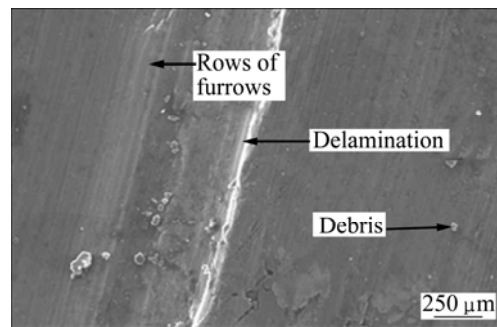


Fig. 10 Wear surface of composite with 3% mica reinforcement under load of 9.81 N and sliding speed of 0.837 m/s

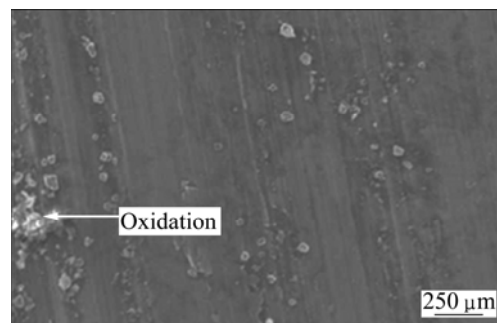


Fig. 11 Wear surface of composite with 3% mica reinforcement under load of 28.43 N and sliding speed of 0.314 m/s

signs of plastic deformation, as seen in Figs. 9–11. The wear track shows clearly the presence of oxide film, which suggests that the relative motion between pins and disc surface generates frictional heat, which significantly affects the wear rate of pins. The results are in agreement with the results of SRINIVASAN et al [27] who found the dominance of oxidative wear at ambient temperature. These are distributed evenly throughout the worn surface and eventually broke off to become debris. The frictional heat during the wear contributes to oxidation of the finer debris more easily than the coarser ones.

4 Conclusions

1) The stir casting method is found to be suitable to fabricate the hybrid aluminium-mica reinforced metal matrix composites.

2) A good bonding between the Al alloy matrix, 10% of SiC and mica reinforcements is observed in the micrograph.

3) Al/10SiC–3mica composites show the maximum strength and hardness.

4) Mica reinforced composites exhibits less wear loss and higher density compared with the ceramic reinforced composites. The results of the ANOVA indicated that load is the main parameter, which influences the wear loss of composites followed by mass fraction of mica.

References

- [1] LEE J A, MYKKANEN D L. Metal and polymer matrix composites [M]. Park Ridge: Noyes Data Corporation.
- [2] JUNG S W, NAM H W, JUNG C K, HAN K S. Analysis of temperature dependent thermal expansion behavior of $\text{SiC}_p/\text{Al}_2\text{O}_3/\text{Al}$ composites [J]. Journal of KSCM, 2003, 16(1): 1–12.
- [3] MATA M, ALCALA J. The role of friction on sharp indentation [J]. Journal of the Mechanics and Physics of Solids, 2004, 52: 145–165.
- [4] ZHAN Y, ZHANG G. Graphite and SiC hybrid particles reinforced copper composite and its tribological characteristic [J]. Journal of Mater Science Letters, 2003, 22: 1087–1089.
- [5] LIANG Y H, WANG H Y, YANG Y F, WANG Y Y, JIANG Q C. Evolution process of the synthesis of TiC in the Cu–TiC–C system [J]. Journal of Alloy of Compounds, 2008, 452: 298–303.
- [6] MATSUNAGA T, KIM J K, HARD CASTLE S, ROHATGI P K. Casting characteristics of aluminium alloy, fly ash composites [J]. Transactions of AFS, 1996, 104: 1097–1102.
- [7] THAKUR S K, KWEE G T, GUPTA M. Development and characterization of magnesium composites containing nano-sized silicon carbide and carbon nanotubes as hybrid reinforcements [J]. Journal of Material Science, 2007, 42: 10040–10046.
- [8] PRASAD R, ASTHANA. Aluminum metal-matrix composites for automotive applications' tribological considerations [J]. Tribol Letters, 2006, 17: 445–453.
- [9] DEONA T H, ROHATGI P K. Cast aluminium alloy composites containing copper-coated ground mica particles [J]. Journal of Material Science, 1981, 16: 1599–1606.
- [10] JHA A K, DAN T K, PRASAD S V, ROHATGI P K. Aluminium alloy solid lubricant talc particle composites [J]. Journal of Material Science, 1986, 21: 3681–3685.
- [11] RAJMOHAN T, PALANIKUMAR K. Modeling and analysis of performance in drilling hybrid composites [J]. The International Journal of Advanced Manufacturing Technology, 2012, DOI: 10.1007/s00170-012-4083-6.
- [12] RAJMOHAN T, PALANIKUMAR K. Experimental investigation and optimization in drilling hybrid aluminium metal matrix composites [J]. Transactions of Nonferrous Metals Society of China, 2012, 22: 1286–1298.
- [13] GENG Lin, ZHANG Hong-wei, LI Hao-ze, GUAN Li-na, HUANG Lu-jun. Effects of Mg content on microstructure and mechanical properties of SiC_p/Al -Mg composites fabricated by semi-solid stirring technique [J]. Transactions of Nonferrous Metals Society of China, 2010, 20: 1851–1855.
- [14] CURLE U A, ANCHEV L. Wear of semi-solid rheo cast SiC_p/Al metal matrix composites [J]. Transactions of Nonferrous Metals Society of China, 2010, 20: 852–856.
- [15] SONG Min. Effects of volume fraction of SiC particles on mechanical properties of SiC/Al composites [J]. Transactions of Nonferrous Metals Society of China, 2009, 19: 1400–1404.
- [16] AMIRKHANLOU S, NIROUMAND B. Synthesis and characterization of 356- SiC_p composites by stir casting and compo casting methods [J]. Transactions of Nonferrous Metals Society of China, 2010, 20: 788–793.
- [17] WANG Yi-qi, SONG Jung-il. Dry sliding wear behavior of Al_2O_3 fiber and SiC particle reinforced aluminium based MMCs fabricated by squeeze casting method [J]. Transactions of Nonferrous Metals Society of China, 2011, 21: 1441–1448.
- [18] GUAN Na, GENG Lin, ZHANG Hong-wei, HUANG Lu-jun. Effects of stirring parameters on microstructure and tensile properties of ($\text{Al}_{70}\text{Mg}_{30}$ + SiC_p)/6061Al composites fabricated by semi-solid stirring technique [J]. Transactions of Nonferrous Metals Society of China, 2011, 21: 274–279.
- [19] ZHAO Long-zhi, ZHAO Ming-juan, YAN Hong, CAO Xiao-ming, ZHANG Jin-song. Mechanical behavior of SiC foam-SiC particles/Al hybrid composites [J]. Transactions of Nonferrous Metals Society of China, 2009, 19: 547–551.
- [20] RICHARD A. FLINN fundamentals of metal casting [M]. USA: Addison Wesley Series in Metallurgy and Materials, 1963: 11–32.
- [21] BASAVARAJAPPA S, CHANDRAMOHAN G, MUKUND K, ASHWIN M, PRABU M. Dry sliding wear behavior of Al 2219/ SiC_p -Gr hybrid metal matrix composites [J]. Journal of Materials Engineering and Performance, 2009, 15: 668–674.
- [22] SONGMENE V, BALAZINSKI M. Machinability of graphitic metal matrix composites as a function of reinforcing particles [J]. Ann CIRP, 1999, 48: 77–80.
- [23] SAHIN Y. Preparation and some properties of SiC particle reinforced aluminium alloy composites [J]. Materials and Design, 2003, 24: 671–679.
- [24] BOWDEN, TABOR D. Friction and lubrication in solids [M]. UK: Oxford University Press, 1981.
- [25] DHARMALINGAM S, SUBRAMANIAN R, SOMASUNDARA VINOTH K. Analysis of dry sliding friction and wear behavior of aluminum–alumina composites using Taguchi's techniques [J]. Journal of Composite Materials, 2010, 44: 2161–2177.
- [26] SONG J I, HAN K S. Effect of volume fraction of carbon fibers on wear behavior of Al/Al, OJC hybrid metal matrix composites [J]. Composite Structures, 1997, 39: 309–318.
- [27] SRINIVASAN M, LOGANATHAN C, KAMARAJ M, NGUYEN Q B, GUPTA M, NARAYANASAMY R. Sliding wear behaviour of AZ31B magnesium alloy and nanocomposite [J]. Transactions of Nonferrous Metals Society of China, 2012, 22: 60–65.

混合铝基复合材料的力学性能和耐磨性

T. RAJMOHAN¹, K. PALANIKUMAR², S. RANGANATHAN³

1. Sri Chandrasekharendra Saraswathi Viswa Maha Vidyalaya University, Enathur, Kanchipuram-631561, India;

2. Sri Sai Ram Institute of Technology, Chennai-600 044, India;

3. Department of Mechanical Engineering, Saveetha School of Engineering, Saveetha University, Chennai-602105, India

摘要: 混合金属基复合材料是重要的工程材料,因为他们比纯铝具有更低的密度、更高的比强度和更好的物理力学性能而广泛应用于汽车、航空航天等方面。研究了混合铝金属基复合材料的力学性能和磨损性能。通过搅拌铸造将云母和 SiC 颗粒加入到 Al 356 合金中。采用扫描电子显微镜(SEM)研究样品的显微组织,用能谱分析(EDX)其化学成分。结果表明,所制备的 Al/10SiC-3 云母复合材料具有较好的强度和硬度。增加复合材料中云母含量能提高复合材料的耐磨性。

关键词: 混合金属基复合材料; SiC; 云母; Al 356 合金; 搅拌铸造; 磨损损失

(Edited by Hua YANG)